UNIVERSIDADE DE SÃO PAULO

INSTITUTO DE FÍSICA
CAIXA POSTAL 20516
01498 - SÃO PAULO - SP
BRASIL

PUBLICAÇÕES

IFUSP/P-890

EXPERIMENTAL SOLID ANGLE CORRECTION FOR GAMMA ANGULAR CORRELATIONS

V.L.C. Procida Veissid, G. Kenchian and M.T.F. da Cruz
Instituto de Física, Universidade de São Paulo

Fevereiro/1991

EXPERIMENTAL SOLID ANGLE CORRECTION FOR GAMMA ANGULAR CORRELATIONS

V.L.C. Procida Veissid, G. Kenchian and M.T.F. da Cruz

Instituto de Física da Universidade de São Paulo
01000 São Paulo, Brazil

Submitted to Nuclear Instruments and Methods in Physics Research, part A

PACS numbers

29.30.Kv

23.20.En

A new method is described for performing solid angle corrections on gamma angular correlation data. The gamma scanning technique was applied to two wrap around Ge(Li) detectors in order to map their intrinsic photopeak efficiencies as functions of the energy and direction of incidence. A collimated ^{152}Eu radioactive source of 1 mCi was used in the mapping procedure. Concerning directional correlations, no numerical integration is necessary for each gamma cascade measured, because a different correlation function is proposed for the fitting, where the angle–dependent effects to be corrected have been factorized. Only a few energy interpolations are needed, in order to obtain the correction coefficients present in the new function. Tests were performed with the 4–2–0 cascade of ^{60}Ni , and 0'–2–0 and 2'–2–0 of ^{100}Ru , showing good agreement with previous results.

1. Introduction

During the past few years, the making of large semiconductor detectors for gamma radiation, with active volumes ranging from about 50 cm^3 to more than 100 cm^3, caused some factories to abandon the true coaxial design, the wrap around type, also known as closed end, being the preferred one. The former is usual in angular correlation experiments, due to its relatively sharp definition of pulse rise times at the preamplifier output, almost independent of where the photon absorption took place. Nevertheless, some of the new detectors do not even have the dimensions of their external and rear contacts quoted in the manuals, depending on the factory. These dimensions are essential if the solid angle corrections are to be calculated using Monte Carlo methods [1,2]. Although other methods might well be applied [3], all of them but the gamma scanning technique adopt hypotheses like: (i) detector perfectly cylindrical (concerning dimensions and internal properties) and (ii) detector aligned and centered inside its end cup. Besides, the use of recovering cryogenic solid state detectors from neutron damage and vacuum faults always changes appreciably their active volumes, what can be easily verified by measuring their new peak–to–Compton ratios. In these cases, gamma scanning is the only way to determine where in the crystal, and how much the efficiency has changed, reenabling these detectors for use in gamma directional correlations.

Although time consuming, scanning the detectors is the only way to produce solid angle corrections reliable until precisions of a fraction of percent for the anisotropy coefficients, as demonstrated in the work of de Bruijn and Lourens [4]. However, when fitting angular correlation data, those authors had thrown away parts of the correlation function that should contain asymmetry and misalignment effects, retaining only the cylindrically symmetric functions. The contribution of these to the final results can be appreciable at that level of precision, as we intend to demonstrate here.

Our purpose is to show a new treatment of the efficiency mapping data, based upon

their expansion in spherical harmonics, and to suggest a new function for fitting angular correlations, where the efficiencies appear completely factorized, with no need of numerical integrations for each cascade analyzed, and with covariances taken into account. This method is useful, regardless of detector shape, size, asymmetry and misalignment relative to the end cup. Damage recovered detectors also belong to this category.

2. The angular correlation function

The experimentally observed angular correlation function, i.e. the number W of coincidences measured as a function of the angle θ between the detectors, for a particular setup and counting time is

$$W(\theta) = Sy_{12} \sum_{\substack{k=0 \\ \text{even}}}^{4} A_{kk} \int_{det1} \frac{d\Omega_1}{4\pi} \int_{det2} \frac{d\Omega_2}{4\pi} \varepsilon_1(E_1,\Omega_1)\, \varepsilon_2(E_2,\Omega_2)\, P_k(\cos\phi_{12}) \quad , \qquad (1)$$

where S is the number of disintegrations of parent nuclei, leading to excited states in the nucleus under study, during the counting time. y_{12} is the yield of the pair γ_1–γ_2 per disintegration. A_{kk} are the anisotropy coefficients, with $A_{00} = 1$. The integration on the direction $\Omega_i \equiv (\theta_i,\phi_i)$ runs over the active volume of the i–th detector, with $\varepsilon_i(E_j,\Omega_i)$ being its intrinsic photopeak efficiency to photons of energy E_j, in the direction of incidence Ω_i. P_k are the Legendre polynomials of order k, and ϕ_{12} is the angle between $d\Omega_1$ and $d\Omega_2$ (see figure 1).

The k=0 term can be brought into evidence in eq.(1), thus producing

$$W(\theta) = \alpha_0 \left[1 + \sum_{\substack{k=2 \\ \text{even}}}^{4} A_{kk}\, F_k(\theta) \right] \quad , \qquad (2)$$

with

$$F_k(\theta) = \frac{\int\int d\Omega_1\, d\Omega_2\, \varepsilon_1(E_1,\Omega_1)\, \varepsilon_2(E_2,\Omega_2)\, P_k(\cos\phi_{12})}{\int\int d\Omega_1\, d\Omega_2\, \varepsilon_1(E_1,\Omega_1)\, \varepsilon_2(E_2,\Omega_2)} \qquad (3)$$

and

$$\alpha_0 = Sy_{12} \int\int \frac{d\Omega_1}{4\pi} \frac{d\Omega_2}{4\pi}\, \varepsilon_1(E_1,\Omega_1)\, \varepsilon_2(E_2,\Omega_2) \quad . \qquad (4)$$

α_0 would be the mean number of counts in case of an isotropic correlation.

In order to evidence the presence of θ on the right side of eq.(3) and factorize it we have to (i) reinterpret $\varepsilon_2(E_2,\Omega_2)$ in the following way: choosing the end cup of detector 1 with its axis coincident with one of the coordinate axes, say 1, $\varepsilon_1(E_1,\Omega_1)$ is measured. $\varepsilon_2(E_2,\Omega_2)$ has to be measured with detector 2 at the same orientation, and as this detector is rotated by the angle θ, what enters eqs.(1)–(4) is, in fact, $\varepsilon^{(\theta)}_{2rot}(E_2,\Omega_2)$, which is the rotated directional efficiency; (ii) to eliminate ϕ_{12} with the help of the addition theorem for spherical harmonics: expressing $P_k(\cos\phi_{12})$ in terms of spherical harmonics on the directions Ω_1 and Ω_2 causes the multiple integrals to separate, and eq.(3) can be rewritten

$$F_k(\theta) = \frac{\sum_{m=-k}^{k} \int d\Omega_1\, \varepsilon_1(E_1,\Omega_1)\, Y_{km}(\Omega_1) \int d\Omega_2\, \varepsilon^{(\theta)}_{2rot}(E_2,\Omega_2)\, Y^*_{km}(\Omega_2)}{(2k+1) \int d\Omega_1\, \varepsilon_1(E_1,\Omega_1)\, Y_{00}(\Omega_1) \int d\Omega_2\, \varepsilon^{(\theta)}_{2rot}(E_2,\Omega_2)\, Y^*_{00}(\Omega_2)} \quad , \qquad (5)$$

where the $Y_{00}(\Omega_i)$ were introduced for convenience. It can be seen that these integrals are the coefficients $\varepsilon_{kmi}(E_j)$ of expansions of the $\varepsilon_i(E_j,\Omega_i)$ in spherical harmonics, namely

$$\varepsilon_i(E_j,\Omega_i) = \sum_{k=0}^{\infty} \sum_{m=-k}^{k} \varepsilon_{kmi}(E_j)\, Y^*_{km}(\Omega_i) \quad , \qquad (6)$$

and we have

$$F_k(\theta) = \frac{\sum_{m=-k}^{k} \varepsilon_{km1}(E_1)\cdot\varepsilon^{(\theta)*}_{km2\,rot}(E_2)}{(2k+1)\ \varepsilon_{001}(E_1)\ \varepsilon^{(\theta)*}_{002\,rot}(E_2)} \quad ; \qquad (7)$$

and finally (iii) to explicitate the active rotation of the $\varepsilon_{km2}(E_2)$: since the $\varepsilon_{km}(E)$, for fixed k, are the components of a tensor of rank k, their rotations can be expressed in terms of the Wigner functions, $D^k_{mm'}$, as follows

$$\varepsilon^{(\alpha\beta\gamma)}_{km\ rot}(E) = \sum_{m'=-k}^{k} \varepsilon_{km'}(E)\ D^k_{mm'}(\alpha\beta\gamma) \quad , \qquad (8)$$

where $(\alpha\beta\gamma)$ are the Euler angles, and their expression in terms of the rotation angle θ depends on the choice of the coordinate axes 1, 2 and 3, in figure 1. Instead of the usual choice $(2,3,1) \equiv (x,y,z)$, we can take $(1,2,3) \equiv (y,-x,z)$ and the Euler angles become $(\alpha\beta\gamma) \equiv (\theta 00)$. The corresponding $D^k_{mm'}$ happens to be only a phase, $e^{im\theta}$, with m=m' and (7) is written

$$F_k(\theta) = \frac{1}{2k+1} \cdot \frac{\sum_{m=-k}^{k} \varepsilon_{km1}(E_1)\ \varepsilon^*_{km2}(E_2)\ e^{-im\theta}}{\varepsilon_{001}(E_1)\ \varepsilon_{002}(E_2)} \quad . \qquad (9)$$

The condition of $F_k(\theta)$ being real imposes the usual connection between $\varepsilon_{km}(E)$ and $\varepsilon^*_{k,-m}(E)$, and the final expression for $W(\theta)$ is

$$W(\theta) = \alpha_0\left[1 + \sum_{\substack{k=2 \\ \text{even}}}^{4} A_{kk} \sum_{m=0}^{k} \frac{2}{(1+\delta_{m0})} (C_{km} \cos m\theta + S_{km} \operatorname{sen} m\theta)\right] \quad , \qquad (10)$$

where

$$C_{km} = \frac{R_{km}}{R_{00}} \qquad \text{and} \qquad S_{km} = \frac{I_{km}}{R_{00}} \quad , \qquad (11)$$

with

$$R_{km} = Re\varepsilon_{km1}(E_1)\ Re\varepsilon_{km2}(E_2) + Im\varepsilon_{km1}(E_1)\ Im\varepsilon_{km2}(E_2)$$

$$I_{km} = Im\varepsilon_{km1}(E_1)\ Re\varepsilon_{km2}(E_2) - Im\varepsilon_{km2}(E_2)\ Re\varepsilon_{km1}(E_1) \quad , \qquad (12)$$

where Re and Im stand for the real and imaginary parts of the ε_{kmi}, respectively. Eq.(10) is the proposed function for fitting the experimental data.

3. Experimental details

The radioactive source was prepared from 21 mg of 97.7% enriched ^{151}Eu, sealed in a quartz capsule. It was irradiated at the nuclear reactor of the Instituto de Pesquisas Energéticas e Nucleares, IPEN, with a neutron flux of $10^{13}\ cm^{-2}\cdot s^{-1}$ during 5 hours, and the resulting activity was of about 1 mCi. This source was inserted in a lead collimator 5 cm thick when viewed from the detector. The photon beam was collimated by a hole of 2 mm in diameter.

The collimator was assembled in a setup able to vary the incidence angles α and β (see figure 2) of the photon beam on the detector. The radioactive source was situated at the origin of the coordinate system, the same position used in angular correlation measurements.

The source to detector end cup distance was 7.00(5) cm and the scanning was made by measuring 269 points on the (α,β) domain, with $\Delta\alpha = \Delta\beta = 2.5^{o}$ (see figure 3). Two Ge(Li) detectors from PGT, with 57 and 61 cm^3 were scanned, each position being measured during 8.5 min of live time.

The electronics was the usual one: an ORTEC 572 amplifier with 2 μs of shaping time, ORTEC 800 analog to digital converter gated in anticoincidence with the pile–up detector circuit of the amplifier, a CAMAC system to account for the live time and accomplish the acquisition in the memory of a PDP 11/84 computer, where 538 spectra of 2048 channels were recorded. The analysis of these spectra was done in a semi–automatic manner, by using IDEFIX code [5], able to fit a multiplet with up to twenty photopeaks, taking into account the background, exponential tails and other charge collection effects, together with calibrations of energy and FWHM. Transitions following the decay of ^{152}Eu were only considered with intensities greater than 2%, relative to the 1408 keV photon [6], an exception being the 1528 keV transition, lying in a clean region of the spectrum.

4. Treatment of the data

A. The efficiency mapping

Once determined the peak areas, these were corrected for the transparency of the collimator due to the exponential law of photon absorption, which is energy dependent. This correction was based upon the peak areas for points in the (α,β) mesh lying outside the crystal, and was relevant for photon energies above 700 keV.

The real and imaginary parts of the $\varepsilon_{km}(E)$ for the considered transitions of ^{152}Sm and ^{152}Gd were calculated by means of a numerical integration, for $k = 0, 2, 4$ and $m = 0, 1, ..., k$ using

$$\left\{ \begin{matrix} Re \\ Im \end{matrix} \right\} \varepsilon_{km}(E) = \sqrt{\frac{(k-m)!}{(k+m)!}} \frac{1}{y(E)} \sum_{ij} A(E,\theta_i,\phi_j)\, P_{km}(\cos\theta_i)\, \text{sen}\,\theta_i \begin{bmatrix} \cos m\theta_j \\ \text{sen}\, m\theta_j \end{bmatrix} p_i\, p_j \ , \tag{13}$$

where $y(E)$ is the relative intensity of photons of energy E, $A(E,\theta_i,\phi_j)$ is the corrected area of the photopeak of energy E, when the collimator pointed to the direction (θ_i,ϕ_j). P_{km} are the associated Legendre polynomials, and p_i, p_j are the Simpson integration weights for the coordinates θ and ϕ. For km fixed, the several $\varepsilon_{km}(E)$ can be fitted by smooth functions of the energy. An example is shown in figure 4. Due to their diverse behaviour for different km pairs, three functions were needed in order to fit the whole ε_{km} set:

$$\ln Z_{km} = a(\ln E)^2 + b(\ln E) + c \ , \tag{14a}$$

$$\ln (-Z_{km}) = a(\ln E)^2 + b(\ln E) + c \ , \tag{14b}$$

and

$$Z_{km} = a E^2 + b E + c \quad , \tag{14c}$$

where a, b and c are the fitting parameters, and Z_{km} stands for the real or imaginary parts of ε_{km}. For the first and second functions proposed it is recommended the use of $\ln(E/E^*)$ instead of $\ln E$, where E^* is approximately the center of the energy interval being adjusted. This procedure contributes to an important reduction of the covariances between the fitting parameters.

B. The angular correlation function

The fitting of angular correlation data is achieved by first interpolating the whole ε_{km} set (15 coefficients, when taking into account the real and imaginary parts) for both gamma energies of the cascade. The R_{km} and I_{km} (eqs.(12)) are then calculated, along with their covariance matrix $\mathbf{M}_{RI}$, and inserted in the proposed fitting function (eq.(10)).

In order to avoid the direct determination of α_0, the relative experimental values $\omega_i = W_i/W_1$, $i = 2, ..., N$, are the ones to be fitted. Their $(N-1) \times (N-1)$ covariance matrix $\mathbf{M}_{\omega exp}$ is given by

$$\mathbf{M}_{\omega exp} = \tilde{\mathbf{T}}_{W\omega}\, \mathbf{M}_{Wexp}\, \mathbf{T}_{W\omega} \quad , \tag{15}$$

where $\left\{\mathbf{M}_{Wexp}\right\}_{ij} = \sigma_i^2\, \delta_{ij}$, $i, j = 1, ..., N$, and $\mathbf{T}_{W\omega}$ is the usual Jacobian transformation matrix [7], the tilde meaning transposition. Likewise, $\mathbf{M}_{RI}$ can be transformed to $\mathbf{M}_{\omega teo}$, a covariance matrix of the relative function at the measured angles, $\omega(\theta_i) = W(\theta_i)/W(\theta_1)$. It represents the contribution to the covariances coming from the scanning procedure. A total covariance matrix $\mathbf{M}_{\omega}$ can then be obtained by adding up $\mathbf{M}_{\omega exp}$ and $\mathbf{M}_{\omega teo}$, since their contributions come from independent sources.

The final step is the minimization of χ^2 with respect to δ, the multipole mixture, directly. This is a covariant χ^2 problem,

$$\chi^2 = \tilde{\Delta}\, \mathbf{M}_{\omega}^{-1}\, \Delta \quad , \tag{16}$$

where Δ is the difference column vector, with elements

$$\Delta_i = \omega_i - \omega(\theta_i) \quad , \quad i = 2, ..., N \quad . \tag{17}$$

The χ^2 minima can now be looked for by means of calculating the $\chi^2 = \chi^2(\delta)$ function, which can be plotted against $\arctan\delta$, as the example in fig. 5. The plausible δ value is the one associated to the deepest minimum, χ^2_{min}, and its standard deviation is taken from the ends of the interval around $\delta(\chi^2_{min})$ where $\chi^2 = \chi^2_{min} + 1$.

5. Applications and discussion

The mapping procedure revealed many features concerning internal and external properties of the detectors: the efficiencies showed some departure from cylindrical symmetry, where differences of up to 10% were measured, mainly at photon energies around 1 MeV. Crystal to end cup misalignments of approximately 3 mm were found for both detectors examined. The data were also able to show the efficiency drop due to the central rear contact, in the range of 10% to 15% when going from 0.1 to 1 MeV photon energies.

The recent angular correlation work of G.Kenchian [8] on ^{100}Rh decay made available a large quantity of data that were analyzed by the traditional method and the one described here, with satisfactory results.

Three gamma cascades from ^{60}Ni and ^{100}Ru are presented, their anisotropy coefficients given in table 1, with additional information. Although the counting statistics attained in these applications do not reach standard deviations of the order of those in ref. 4, the results agree well with the expected ones, even for the $2' \longrightarrow 2$ transition in ^{100}Ru , since the mean value of the multipole mixture for several independent correlations produced 3.70(41) , in close agreement with older data [9].

As a final remark, eq.(7) for the $F_k(\theta)$ could be seen as a matrix product,

$$F_k(\theta) \;\; \alpha \;\; \varepsilon^{\dagger}_{k2} \; D^{k\dagger} \; \varepsilon_{k1} \qquad (18)$$

where the ε_{ki} are column vectors and D^k is the rotation matrix. The choice of axes permitted to diagonalize D^k, but keeping the asymmetry effects imply to maintain all the nonzero m products (especially the odd–m components) in eq.(18). Their relative weights, namely the C_{km} and S_{km} coefficients of eq.(10) can be appreciated from table 2,

for the first cascade in table 1. These numbers show that, in our experimental setup, they must be all present in order for us to achieve reliable anisotropy coefficients at the precision of a fraction of percent. Needless to point out that if one intends to use noncylindrical detectors (as the recovered ones might become), the correction effects are even more important.

Acknowledgments

The authors wish to thank Dr. I.D. Goldman for his fruitful discussions throughout the development of this work, Dr. R.N. Saxena for yielding the enriched europium target and providing its irradiation, and Drs. P.R. Pascholati and C.T. Yuen for their critical reading of this manuscript.

References

[1] D.C. Camp and A.L. van Lehn, *Nucl. Instrum. Methods* **76**, 192 (1969).

[2] E. Hourany, *Nucl. Instrum. Methods* **94**, 401 (1971).

[3] E. Karlsson, in *Proc. Int. Conf. on Angular Correlations in Nuclear Disintegration*, 1970, edited by H. van Krugten and B. van Nooijen (Rotterdam University Press, Groningen, 1971).

[4] D. de Bruijn and W. Lourens, *Nucl. Instrum. Methods* **178**, 269 (1980).

[5] P. Gouffon, IDEFIX User's Guide, IFUSP internal publication, 1987.

[6] Y. Yoshizawa, Y. Iwata, T. Kaku, T. Katoh, J. Ruan, T. Kojima and Y. Kawada, *Nucl. Instrum. Methods* 174, 109 (1980); ibid. 174, 133 (1980).

[7] L. Lyons, *Statistics for nuclear and particle physicists* (Cambridge University Press, Cambridge, 1986).

[8] G. Kenchian, M. Sc. thesis, IFUSP 1990, to be published.

[9] J. Lange, K. Kumar and J.H. Hamilton, *Rev. Mod. Phys.* **54**, 119 (1982); ibid. **54**, 673 (1982).

Figure Captions

Fig. 1. Geometry of a directional gamma correlation. S is the source position.

Fig. 2. Representation of the gamma scanning angles, α and β.

Fig. 3. Peak area distribution in the (α,β) domain, for detector 1 and photon energy of 122 keV (maximum value is 34600 counts).

Fig. 4. Fitting of $\ln \varepsilon_{00}$ versus $\ln E$.

Fig. 5. Typical plot of $\log \chi^2$ versus $\arctan \delta$.

Table 1

Results obtained in the analysis of gamma directional correlations in ^{60}Ni and ^{100}Ru.

Nuclide	Spin sequence	Gamma energies (keV)	A_{22} and A_{44}
^{60}Ni	4–2–0	1173–1333	0.104(12) 0.009(3)
^{100}Ru	0^{+}–2–0	590–540	0.331(76) 1.06(24)
^{100}Ru	2^{+}–2–0	822–540	$-0.215(8)^{a}$ 0.312(2)

[a] values corresponding to a multipole mixture of 4.55(23), consistent with older data [9].

Table 2

C_{km} and S_{km} coefficients for the 4–2–0 cascade of ^{60}Ni .

km	C_{km}	S_{km}
00	1.0000	——
20	0.2184	——
21	− 0.0020	0.0001
22	0.3273	− 0.0270
40	0.0888	——
41	− 0.0027	0.0001
42	0.0992	− 0.0084
43	− 0.0021	0.0002
44	0.1756	− 0.0296

Figure 1

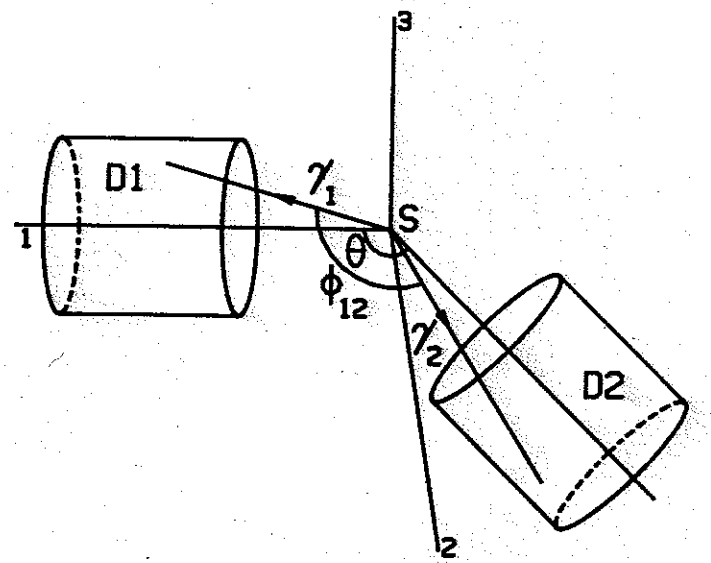

Figure 2

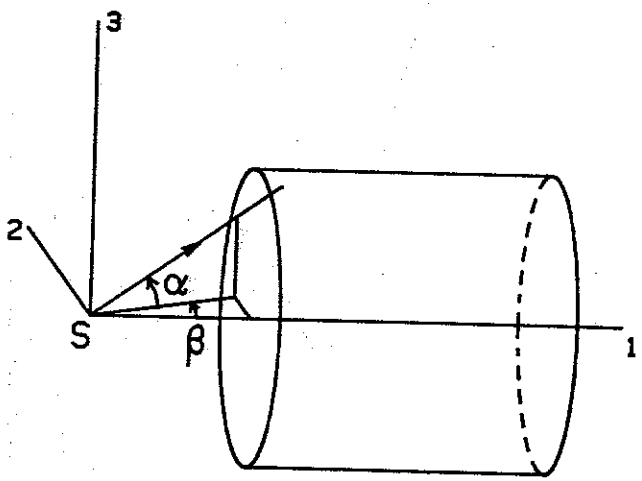

Figure 3

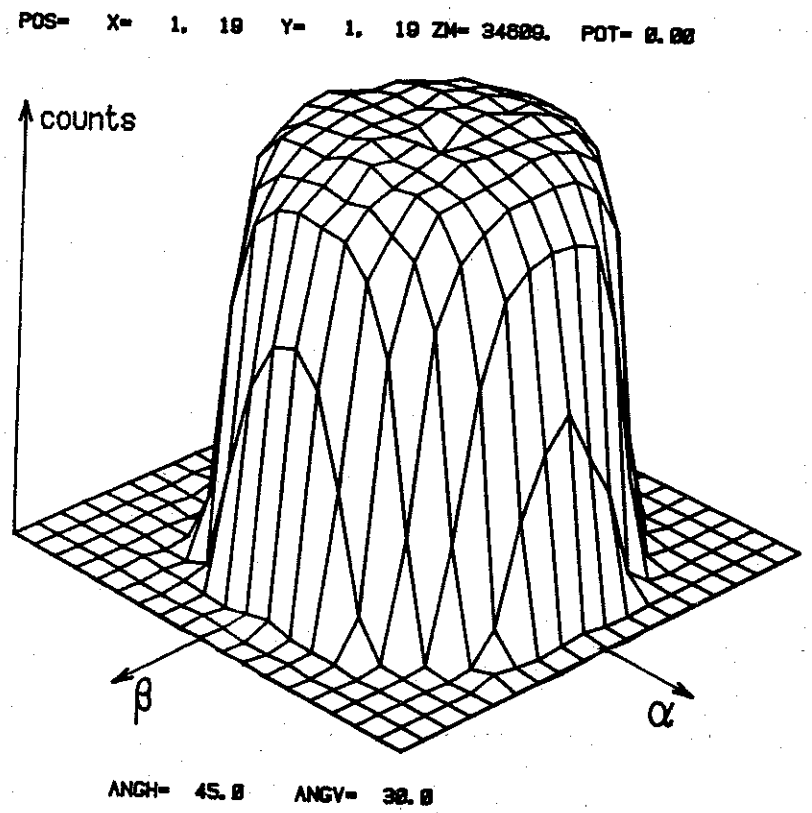

Figure 4

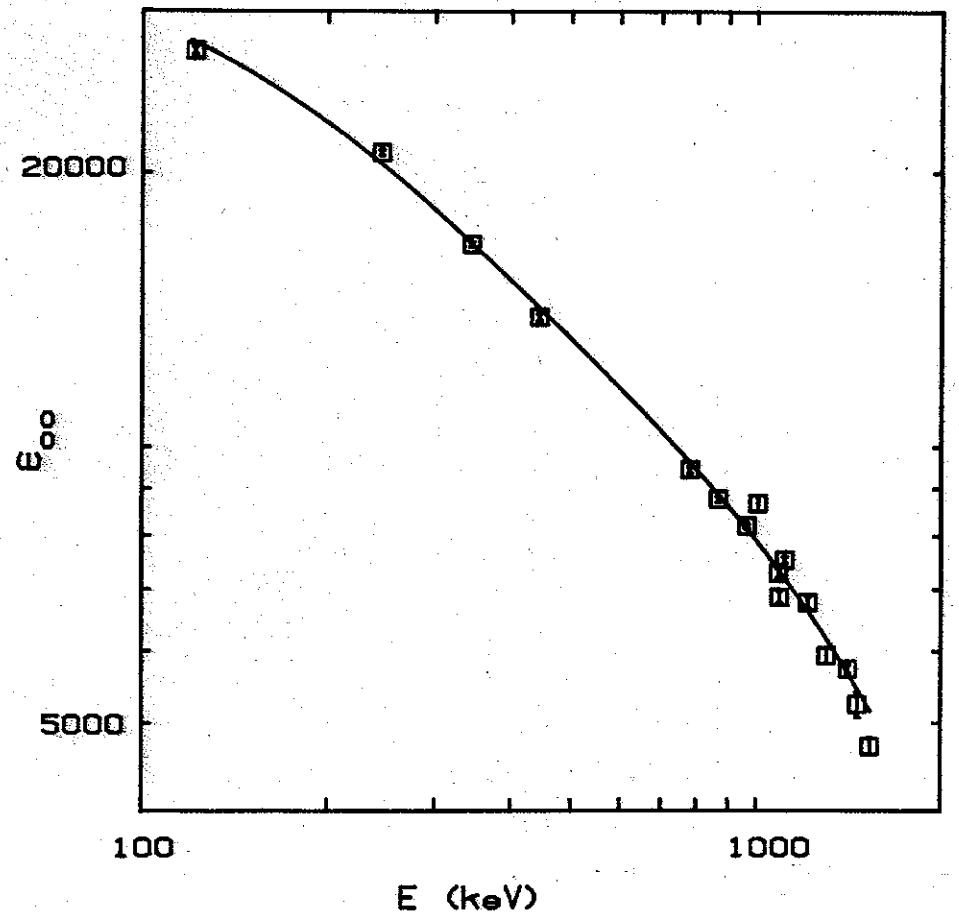

Figure 5